Hubert Chanson
Engineering Consultant,
F75116 Paris, France

Study of Air Demand on Spillway Aerator

1 Introduction

1.1 Presentation. The irregularities on the spillway surfaces will in a high speed flow cause small areas of flow separation. In these regions the pressure will be lowered and if the velocities are high enough the pressure may fall to below the local vapor pressure of the water. Vapor bubbles will form and when they are carried away downstream into high pressure region the bubbles collapse and possible cavitation damage may occur. Experimental investigations (Volkart and Rutschmann (1984)) show that the damage can start at clear water velocities of between 12 to 15 m/s. Up to velocities of 20 m/s the surfaces may be protected by streamlining the boundaries, improving the surface finishes or using resistant materials.

When air is present in the water the resulting mixture is compressible and this damps the high pressure caused by the bubble collapses (Peterka (1953)). Peterka, Russell and Sheehan (1974) performed experiments on concrete specimens and showed that air concentrations of 1–2 percent reduce substantially the cavitation erosion and above 5–7 percent no erosion was observed. When there is not enough surface aeration (i.e., downstream of a gate) or if the tolerances of surface finish required to avoid cavitation are too severe (i.e., V > 30 m/s), air can be artificially introduced by aeration devices (called aerators) located on the spillway floor and sometimes on the side walls.

1.2 Aeration Devices. The design of a small deflection in a spillway structure (i.e., ramp, offset) tends to deflect the high velocity flow away from the spillway surface (Fig. 1). In the cavity formed below the nappe, a local subpressure beneath the nappe (ΔP) is produced by which air is sucked into the flow (Q_{air}^{inlet}).

The properties of the different types of aeration devices were detailed by Vischer et al. (1982). A combination of a ramp, an offset, and a groove provides the best design: the ramp dominates operation at small discharges while the groove provides space for the air supply and the offset enlarges the trajectory of the jet at higher discharges. Volkart and Chervet (1983) have studied on model the behavior of a large range of aerators.

1.3 Mechanisms of Air Entrainment. Chanson (1989) showed that the air entrainment above an aerator (Fig. 2) is characterized by: 1 air entrainment through the upper and lower free surfaces of the water jet called nappe entrainment, 2 plunging jet entrainment at the intersection of the water jet and the rollers, and 3 air recirculation in the cavity below the jet. The study of the different mechanisms of air entrainment is complex because of the interactions between the different air entrainment processes.

The first step is the study of the air demand relationship. The air demand may be defined as the relationship between the air discharge provided by the air supply system, the subpressure in the cavity and its distribution along the nappe, and the flow characteristics. The operating point of a bottom aerator is then obtained by combining the pressure drop curves of the air supply system with the air demand characteristic curves as detailed by Low (1986). This calculation fixes the cavity under pressure, and hence the jet trajectory and the cavity geometry.

Previous authors (Pinto et al. (1982), Tan (1984)) presented the air demand relationship as: $q_{air}^{inlet} = K * L_{jet}$ but this does not take in account the air recirculation and the plunging jet entrainment and it becomes usual (Chanson (1989) and Low (1986)), to study the air demand as: $Q_{air}^{inlet}/Q_w = f(P_N, \text{Fr})$.

1.4 Experiments. The author (Chanson (1988)) performed experiments on a 1:15 scale model of the Clyde dam spillway with a slope $\alpha = 52.33°$. The model provided Froude numbers in the range 3 to 25 with initial average flow velocities from 3 m/s to 14 m/s. By adjusting the gate at the entry of the flume the initial flow depth was from 20 mm to 120 mm. The first aerator configuration included a ramp of 5.7° (t_r = 30 mm, L_{ramp} = 300 mm) and an offset of 30 mm height. This geometry was the same as that used by Low (1986). The second configuration had no ramp and an offset of 30 mm height as

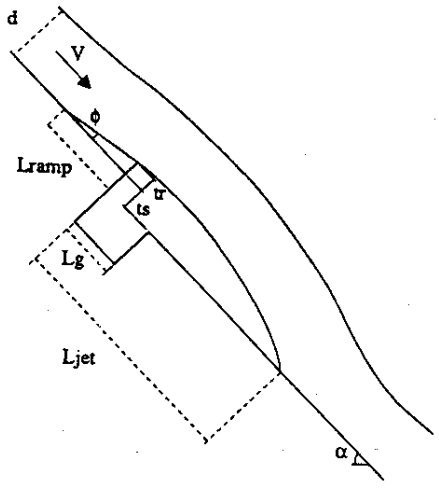

Fig. 1 Geometry of an aerator device

Contributed by the Fluids Engineering Division for publication in the JOURNAL OF FLUIDS ENGINEERING. Manuscript received by the Fluids Engineering Division March 7, 1989.

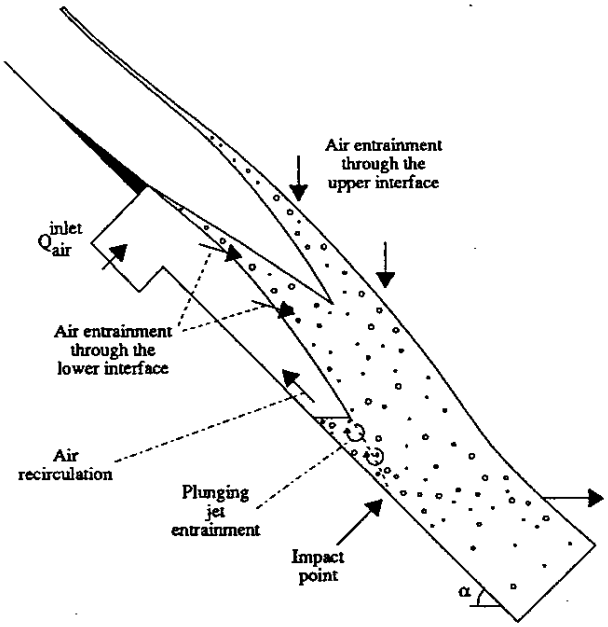

Fig. 2 Air entrainment above an aerator

that used by Tan (1984). The author performed air demand experiments with both aerator configurations. In some cases two fans were connected to the air supply inlets to boost the pressure beneath the nappe to the atmospheric pressure.

First various parameters are detailed, then the experimental results are presented and finally a study of the particular case $Q_{air}^{inlet} = 0$ is developed.

2 Dimensionless Parameters

2.1 Parameters. The relevant parameters needed for any dimensional analysis come from the following groups:

A Fluid Properties. These consist of: the pressure above the flow P_0 (Pa), the density of water ρ_w (kg/m^3), the density of air ρ_{air} (kg/m^3), the dynamic viscosity of water μ (N.s/m^2), the surface tension of the water (N/m), the vapor pressure at the experiment temperature P_v (Pa) and the acceleration of gravity g (m/s^2).

B Spillway and Aerator Geometry. They are: the spillway slope α, the channel width W (m), the roughness of the spillway surface k_s (m), the offset height t_s (m), the groove length L_g (m), the duct area below the spillway surface A_d (m^2), the angle between the ramp and the spillway ϕ and the ramp length L_{ramp} (m).

C Geometry of the Air Inlets.

D Flow Properties. These consist of: the velocity distribution, the air concentration distribution at the end of the approach flow, the distribution of the axial component of turbulent velocity, and the distribution of the lateral component of turbulent velocity. Normally the distributions of these parameters are replaced by their mean value: the water depth of the flow in the approach zone d (m), the flow velocity V (m/s), the root mean square of axial component of turbulent velocity u' (m/s), and the root mean square of lateral component of turbulent velocity v' (m/s).

E Undernappe Cavity Properties. These consist of: the water jet length L_{jet} (m), the difference between atmospheric pressure and air pressure beneath the nappe ΔP (Pa), and the air discharge through the ducts Q_{air}^{inlet} (m^3/s).

F Downstream Flow Properties. These consist of: the air concentration distribution, the flow depth and the velocity distribution downstream of the aerator.

The study on spillway model uses the atmospheric pressure as pressure above the flow and when the vapor pressure P_v is small compare to the atmospheric pressure and the pressure in the cavity ($P_0 - \Delta P$), the parameters P_0 and P_v may be neglected. Laali (1980) performed experiments with variations of the pressure above the flow and his results will be discussed later.

Ervine and Falvey (1987) showed that the lateral component of turbulence intensity v'/V is proportional to the axial turbulence intensity u'/V and for an axisymmetric jet their results fitted: $v'/V = 0.38 * u'/V$. For a two-dimensional plane jet it is reasonable to assume that there will be a similar relationship and this enables us to replace u' and v' by the independent parameter u'.

Nomenclature

A_d = duct area below the surface spillway (m^2)
C = air concentration defined as the volume of air per unit volume
C_{QV} = volume air flow coefficient (13)
d = characteristic depth (m) defined as: $d = \int_0^{y_{90}} (1 - C) * dy$
Eu = Euler number defined as: $\text{Eu} = V/\sqrt{\Delta P/\rho_{air}}$
Fr = Froude number defined as: $\text{Fr} = V/\sqrt{g*d}$
g = gravity constant (m/s^2) - local value: $g = 9.8050$ m/s^2 (Christchurch, New Zealand)
L = distance along the spillway from the end of the deflector (m)
L_{jet} = distance of the impact point of the jet from the end of the deflector (m)
P_{atm} = atmospheric pressure (Pa)
P_o = pressure above the jet (Pa)
P_N = pressure gradient number defined as: $P_N = \Delta P/(\rho_w * g * d)$
Q_{air} = air discharge (m^3/s)
Q_{air}^{inlet} = air discharge provided by the air supply system (m^3/s)
Q_w = water discharge (m^3/s)
q_{air}^{inlet} = air discharge provided by the air supply system per meter width (m^3/s/m)
Re = Reynolds number defined as: $\text{Re} = \rho_w * V * d/\mu$
Sygma = relative subpressure
t_r = ramp height (m)
t_s = offset height (m)
Tu = turbulence intensity defined as: $\text{Tu} = u'/V$
U_w = average water velocity (m/s) defined as: $U_w = q_w/d$
u' = root mean square of axial component of turbulent velocity (m/s)
V = velocity (m/s)
W = channel width (m)
We = Weber number
y = depth measured perpendicular to the spillway surface (m)
α = spillway slope
β^{inlet} = dimensionless air discharge provided by the air supply system
ΔP = difference between the pressure above the flow and the air pressure beneath the nappe (Pa): $\Delta P = Po - Pcavity$
ϕ = angle between the ramp and the spillway
μ = dynamic viscosity of water (N.s/m^2)
ρ_{air} = density of air (kg/m^3)
ρ_w = density of water (kg/m^3)

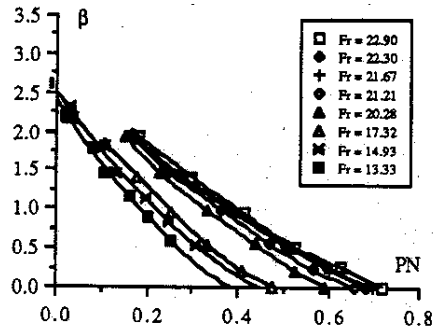

Fig. 3(a) Ramp 5.7° – d/t_s = 0.95

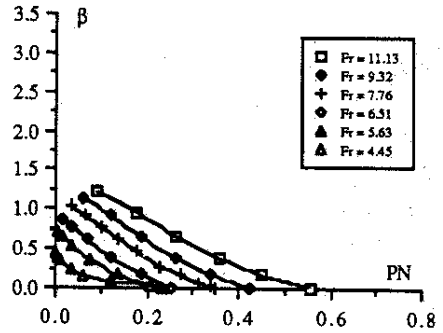

Fig. 3(b) Ramp 5.7° – d/t_s = 2.17

Fig. 3 Characteristic curves—aerator with a 30 mm offset height and a ramp

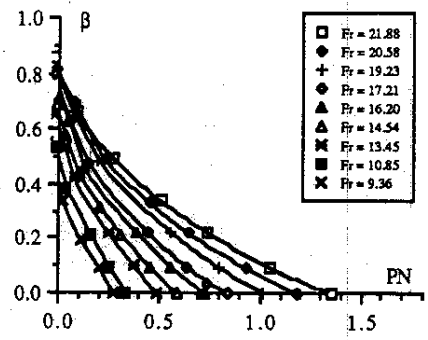

Fig. 4(a) No ramp – d/t_s = 0.95

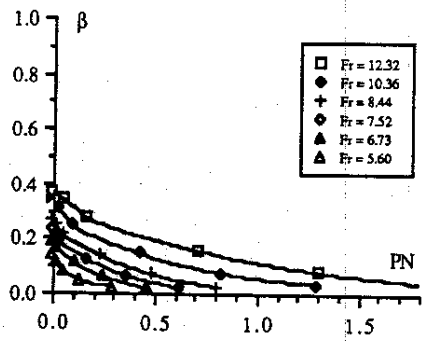

Fig. 4(b) No ramp – d/t_s = 2.17

Fig. 4 Characteristic curves—aerator with a 30 mm offset height

The parameters required to design an aerator are: 1 the air discharge Q_{air}^{inlet}, 2 the air concentration near the floor downstream of the aerator C_b, 3 the difference between the atmospheric pressure and the pressure in the cavity beneath the nappe ΔP and 4 the water jet length L_{jet}. Each of these design parameters is a function of the initial independent parameters:

$$L_{jet}, Q_{air}^{inlet}, \Delta P, C_b = f(\rho_w, \rho_{air}, \mu, \sigma, g, \alpha, W, k_s, t_s, L_g, A_d, \phi, L_{ramp}, V, d, u') \quad (1)$$

2.2 Dimensionless Numbers. The variables above give the following dimensionless numbers: the nondimensional air discharge $\beta^{inlet} = Q_{air}^{inlet}/Q_w$, the air concentration at the bed C_b, the jet length L_{jet}/d, the dimensionless geometric variables k_s/d, t_s/d, L_g/d, $A_d/(d*W)$, L_{ramp}/d, the Froude, Reynolds, Weber and Euler numbers, the density ratio ρ_{air}/ρ_w and the turbulence intensity: Tu = u'/V.

Any combination of these numbers is also dimensionless and may be used to replace one of the combinations. It will be shown later that it is convenient to replace the Euler number by a pressure gradient number P_N defined as

$$P_N = \frac{\Delta P}{\rho_w * g * d}$$

This number is obtained from the others by the relation:

$$P_N = \left(\frac{Fr}{Eu}\right)^2 * \frac{\rho_{air}}{\rho_w}$$

For the study of cavity at the rear of a hydrofoil other workers (Laali and Michel (1984)) have used, in place of the air discharge β^{inlet} and the pressure gradient P_N, 1 the volume air flow coefficient C_{QV} and 2 the relative subpressure Sygma defined as

$$C_{QV} = \frac{Q_{air}^{inlet}}{V * W * (t_S + t_r)} \quad \text{Sygma} = \frac{\Delta P + \rho_w * g * d}{\frac{1}{2} * \rho_w * V^2}$$

The coefficient C_{QV} is equal to the ratio of the mean air velocity in the cavity over the flow velocity in the jet and for vapor cavity ($P_{cavity} = P_v$) the number Sygma equals the cavitation number σ_v. Both coefficients may be deduced from the others:

$$C_{QV} = \beta^{inlet} * \frac{d}{t_s + t_r} \quad \text{Sygma} = 2 * \left(\frac{P_N + 1}{Fr^2}\right)$$

Studies are performed on geometrically similar models and it is convenient to use a slice model. Side effects may appear due to the boundary layers on the side walls. However if these boundary effects are assumed small, the problem becomes a two-dimensional study. The nappe subpressure is usually controlled by valves on the air inlet systems and this enables the underpressure to be treated as an independent parameter. The density ratio is almost constant. From these considerations the relationship (1) is rewritten in terms of dimensionless parameters:

$$\frac{L_{jet}}{d}, \beta^{inlet}, C_b = f\left(\text{Re}, \text{We}, \text{Fr}, \alpha, \frac{k_s}{d}, \frac{t_s}{d}, \frac{L_g}{d}, \frac{A_d}{W*d}, \phi, \frac{L_{ramp}}{d}, \text{Tu}, P_N\right) \quad (2)$$

2.3 Discussion. For a given aerator configuration (α, k_s, t_s, L_g, A_d, ϕ, L_{ramp} fixed) and a given flow depth d, the relationship (2) becomes:

$$L_{jet}/d, \beta^{inlet}, C_b = f(\text{Re}, \text{We}, \text{Fr}, \text{Tu}, P_N) \quad (3)$$

According to Laali (1984), Kobus (1984), and Pinto (1984) the Reynolds and Weber numbers do not influence the processes in any significant way if: 1 the Reynolds number is greater than 10^5 and 2 – the Weber number $W_1 = \frac{V}{\sqrt{\sigma/(\rho_w * L_{jet})}}$ is greater than 400.

The ratio W_1 is defined by Pinto (1984) using the jet length

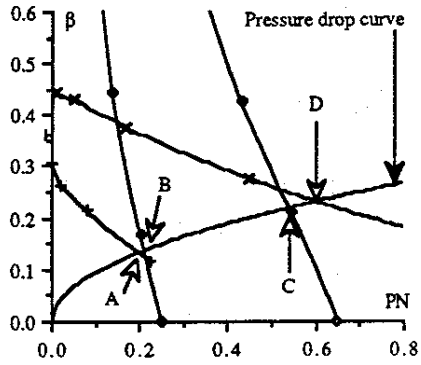

Fig. 5 Influence of the ramp – d/t_s = 1.65
Ramp 5.7°: ◇ Fr = 13.49 ◆ Fr = 7.56
No ramp: × Fr = 13.76 + Fr = 7.47

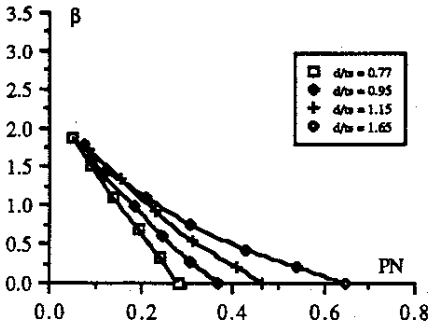

Fig. 6(a) Ramp 5.7° – Fr = 14.5

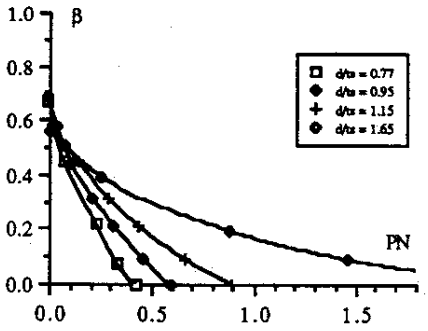

Fig. 6(b) Ramp 5.7° – Fr = 14.7

Fig. 6 Influence of the depth of water on the characteristic curves

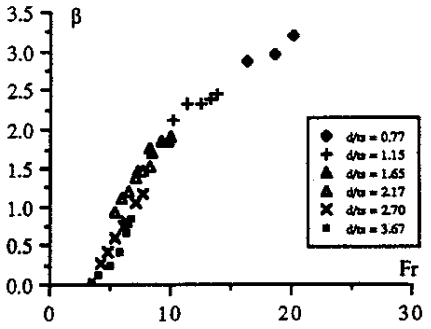

Fig. 7(a) Ramp 5.7° – P_N = 0.0

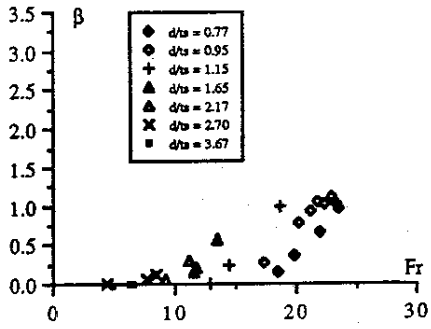

Fig. 7(b) Ramp 5.7° – P_N = 0.4

Fig. 7 Curves $\beta^{inlet} = f(Fr)$—aerator with a 30 mm offset height and a ramp

as characteristic length. Pinto et al. (1982) performed experiments on a series of hydraulic model whose scale varied from 1:8 through to 1:50 and were able to show that the model reproduced the prototype air demand for all water discharges for scales larger than 1:15. For scales 1:30 and 1:50 the correct air demand was only reproduced for the larger discharges. The dimensionless equation (3) then becomes:

$$L_{jet}/d,\ \beta^{inlet},\ C_b = f(\mathrm{Fr},\ \mathrm{Tu},\ P_N)$$

There is little information available on the effects of turbulence. Often the studies neglect the influence of the turbulence intensity (Vischer et al. (1987), Low (1986), and Laali and Michel (1984)) and it then becomes:

$$L_{jet}/d,\ \beta^{inlet},\ C_b = f(\mathrm{Fr},\ P_N) \qquad (4)$$

As discussed earlier the air entrainment above an aerator may occur by different processes. Each of these processes yields a different nondimensional equation and the interactions between these processes must be considered. More the upstream conditions include the air concentration, velocity, turbulence and pressure distributions rather than the average values. Therefore it is believed that the type of relation defined in equation (4) is incomplete and neither does it characterize any single physical process.

The data obtained on the Clyde dam spillway model are analyzed using equation (4) and the equation inadequacy is discussed later.

3 Characteristic Curves

3.1 Results. For different flow depths we measured the characteristic curves $\rho^{inlet} = f(P_N)$ for several Froude numbers (Figs. 3 and 4). It must be noticed that the scales of the graphs are not the same for the two aerator configurations. The relationship between the three dimensionless numbers shows that a decrease of air discharge brings an increase of the nappe subpressure and for the same nappe subpressure the air discharge increases with the Froude number.

Figure 5 shows the air demand curves for two Froude numbers with both aerator geometries and they are compared with a typical pressure drop curve of the air supply system. At low Froude numbers the operating point of the aerator with ramp (point B) shows that this configuration provides a larger air discharge than the aerator configuration without ramp (point A). At high Froude numbers the aerator without ramp (point D) supplies more air than with ramp (point C). This phenomenon occurs because the presence of the ramp increases the slope of the curve $\beta^{inlet} = f(P_N)$ for identical upstream flow conditions.

Figure 6 presents β^{inlet} as function of the initial depth of water d/t_s for constant Froude numbers. The results show that an increase of the flow depth decreases the average slope of $\beta^{inlet} = f(P_N)$, increases the pressure gradient for $\beta^{inlet} = 0$ and decreases the air discharge β^{inlet} when P_N reaches zero. It must be emphasized that we cannot separate the effects of two parameters d/t_s and d/L_{ramp}. For a geometry with ramp, for the same flow depth, increasing the ramp length increases the

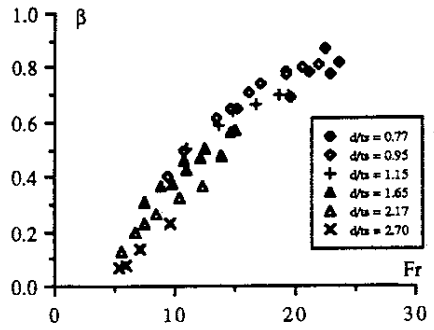

Fig. 8(*a*) No ramp – $P_N = 0$

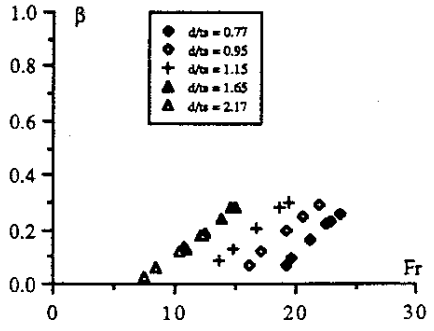

Fig. 8(*b*) No ramp – $P_N = 0.6$

Fig. 8 Curves $\beta^{inlet} = f(Fr)$—aerator with a 30 mm offset height—no ramp

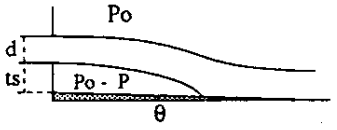

Fig. 9 Half-cavity geometry—Laali (1980)

depth of flow for which the streamlines are parallel to the ramp. Above this depth the streamlines are less affected by the slope.

Another way to present the characteristic curves is by plotting β^{inlet} as a function of the Froude number for constant pressure gradient (Figs. 7 and 8).

3.2 Discussion. Laali performed experiments on a horizontal half-cavity (Fig. 9) within the framework of study of cavity in the rear of hydrofoils. His data were originally plotted as: $C_{QV} = f(\text{Sygma})$ and are presented as $\beta^{inlet} = f(P_N)$ in analogy of the study on spillway model.

The air demand plotted as $\beta^{inlet} = f(P_N)$ has two linear sections connected by a transition zone (Fig. 10). These regions correspond to different air entrainment processes. For low air discharges and low Froude numbers most of the air is evacuated at the rear of the cavity by plunging jet entrainment. For middle values of the air inflow (transition zone) Michel (1984) indicates that plunging jet entrainment becomes insufficient and a pulsation phenomenon may appear which is characterized by evacuation of pockets of air trapped by a re-entrant jet at the rear of the cavity. Similar pulsation phenomena were observed on spillway model Chanson (1988) and on prototype (Frizell (1985)). A hysteresis process occurs at the transition between high and low air discharges: the relationship $\beta^{inlet} = f(P_N)$ has a different shape for increasing and decreasing air supply discharges. All experiments presented (1988; 1980) were performed with a decreasing flow rate to avoid this phenomenon.

For high air discharges most of the air is entrained by nappe entrainment. For large jet lengths and hence for high Froude

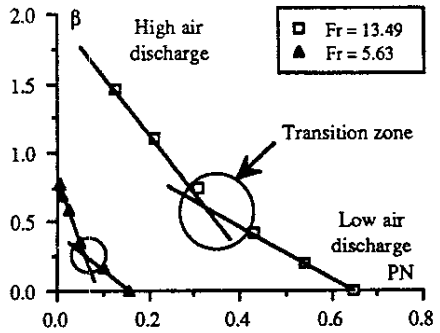

Fig. 10(*a*) Author's data Chanson (1988) ramp 5.7° – $dI t_s = 1.65$

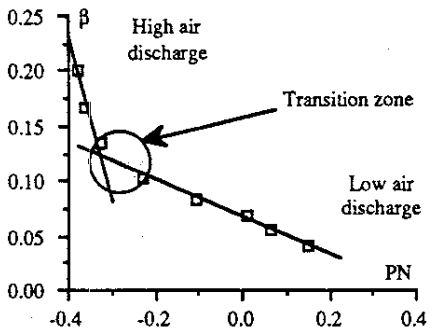

Fig. 10(*b*) Laali (1980) $P_0 = 1.03\ 10^4$ Pa – $dI t_s = 2.05$

Fig. 10 Characteristic curves $\mu^{inlet} = f(P_N)$

Laali's data (1980) $\Delta(P_0) = \pm 73$ Pa $\Delta(\beta^{inlet})/\beta^{inlet} = \pm 2$ percent $\Delta(P_N) = \pm 2$ percent $\Delta(\text{Fr})/\text{Fr} = \pm 0.34$ percent

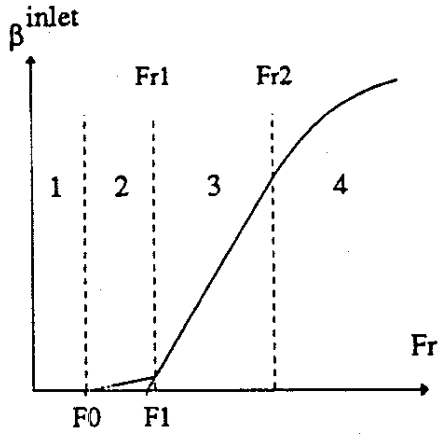

Fig. 11 Scheme of the relation $\beta^{inlet} = f(\text{Fr})$

numbers Laali (1980) suggests that the air-water mixture along the lower interface of the jet tends to block the formation of the re-entrant jet and at the limit the pulsation regime may disappear. This is in agreement with the data obtained on spillway model (Fig. 10(*a*)) that show two different shapes of curve $\beta^{inlet} = f(P_N)$ with the transition zone.

For a given depth of water and aerator geometry, the relationship $\beta^{inlet} = f(\text{Fr})$ for a constant pressure gradient indicates four characteristic regions (Fig. 11). For low Froude numbers (region 1) there is no air entrainment. Observations of the experiments indicate that no air is entrained through the free-surfaces of the jet, and according to Ervine and Ahmed (1982), air entrainment by plunging jet entrainment does not occur below a critical velocity $V_c = 0.8$ m/s. Hence a characteristic Froude number F_0 can be defined such there is no entrainment for: $\text{Fr} < F_0 = V_c/\sqrt{g*d}$.

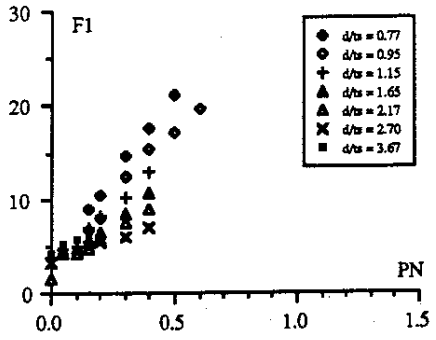

Fig. 12(*a*) Aerator with ramp 5.7°

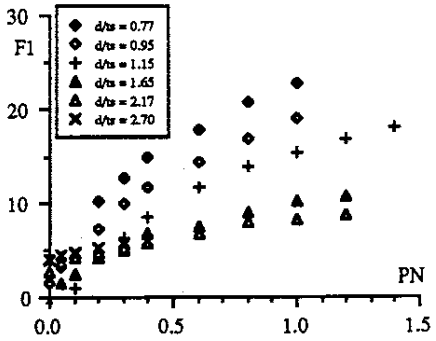

Fig. 12(*b*) Aerator without ramp

Fig. 12 Variations of the characteristic Froude number F_1 $\Delta(F_1) = \pm$ 5 percent

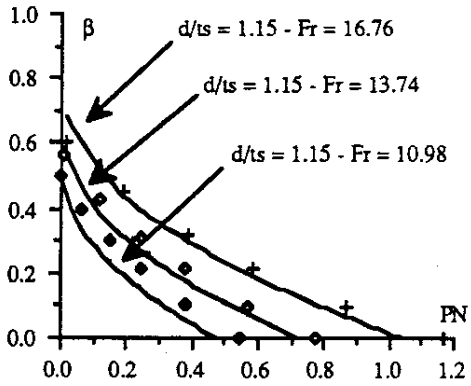

Fig. 13 Comparison between the data and the equation (7) aerator without ramp

In the region 2, most of the air is entrained by plunging jet entrainment and photographs show that no nappe entrainment occurs. Air bubbles are entrapped when the water jet intersects the rollers and dragged away by the flow.

For a high velocity jet nappe entrainment occurs and the air is entrained by high intensity turbulent eddies close to the free-surface. This process occurs in the region 3 and the air is entrained by addition of plunging jet entrainment and nappe entrainment. The latter becomes major for higher Froude numbers. The start of nappe entrainment is well marked and may be characterized by a characteristic Froude number Fr[1]. For a given flow depth and pressure gradient P_N, the relationship $\beta^{inlet} = f(\mathrm{Fr})$ is almost linear in the region 3 and is estimated as:

$$\beta^{inlet} = K_1 * (\mathrm{Fr} - \mathrm{F_1}) \tag{5}$$

At higher Froude numbers (region 4) the air entrainment is limited by the limit air transport capacity of the flow. Kobus

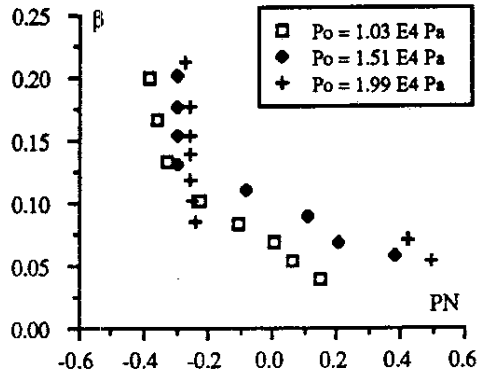

Fig. 14 Influence of the pressure P_0 on air demand—Laali (1980)

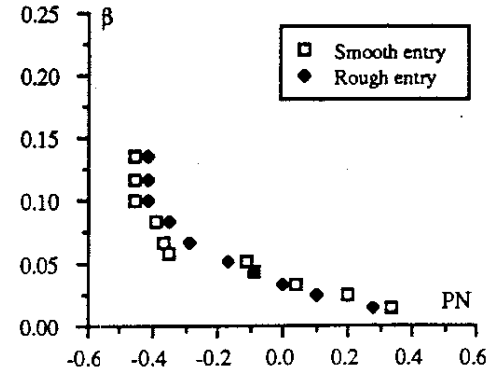

Fig. 15 Influence of the roughness on air demand—Laali (1980)

(1984) and Brauer (1971) indicate that this limit is given by the maximum air bubble concentration in the flow. The relationship $\beta^{inlet} = f(\mathrm{Fr})$ is no longer linear. A statistical study Chanson (1988) suggests:

$$\beta^{inlet} = K_2 * \sqrt{\mathrm{Fr} - \mathrm{F_2}} \tag{6}$$

The change of mechanism of air entrainment observed between the regions 2 and 3 is clearly marked in both aerator geometries for different flow depths, cavity subpressures and flow velocities. To a first approximation the characteristic Froude number F_1 (equation (5)) is assumed to represent the start of nappe entrainment. Variations of F_1 as a function of the depths of water and Froude numbers are shown in Fig. 12 for both geometries. A statistical study of the coefficients K_1 and F_1 Chanson (1988) indicates that in the region 3 (Fig. 11) the air demand characteristic curves $\beta^{inlet} = f(\mathrm{Fr}, P_N)$ are estimated by:

$$\beta^{inlet} = K_1 * (\mathrm{Fr} - f_1 - E_1 * \sqrt{P_N}) \tag{7}$$

where $E_1 = 23.51 * (d/t_s)^{-3/2}$

$f_1 = -8.17 + 5.77 * (d/t_s) - 0.605 * (d/t_s)^2$

$K_1 = 0.2$ (Ramp 5.7° $K_1 = 0.06$ (No ramp)

It must be noticed that the coefficients E_1 and f_1 are independent of the ramp and the characteristic Froude number F_1 is only function of P_N and d/t_s. The equation (7) provides a good fit of the experimental data from the Clyde dam spillway model (Fig. 13) but may not be generally applicable to aerators of differing geometry or different spillway slopes.

3.3 Influence of Other Parameters. Laali (1980) was able to vary parameters as the absolute pressure above the flow P_o and the roughness of the injector. His results are presented on Figs. 14 and 15 and the different flow conditions are reported on Table 1. In the range of considered pressure (10^4 Pa, 2 10^4

Table 1 Laali's experimental configuration

	d m	ts m	θ	Fr	Po
Fig. 10(*b*)	0.1003	0.049	1.87°	8.065	$1.03\ 10^4$
Fig. 14	0.1003	0.049	1.87°	8.065	variable
Fig. 15	0.1389	0.030	3.10°	6.442	$1.41\ 10^4$

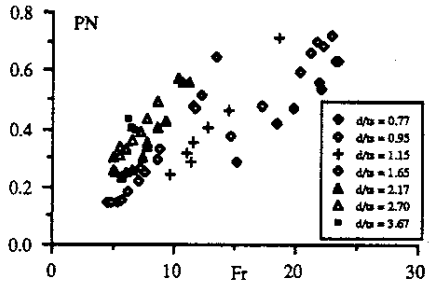

Fig. 16(*a*) Ramp 5.7°

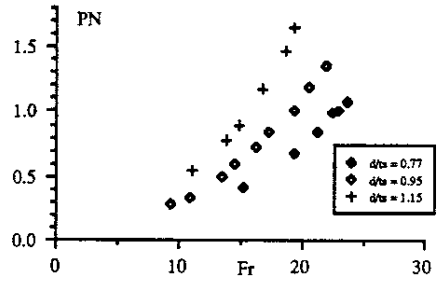

Fig. 16(*b*) No ramp

Fig. 16 Plot of P_N as a function of the Froude number for $Q_{air}^{inlet} = 0$

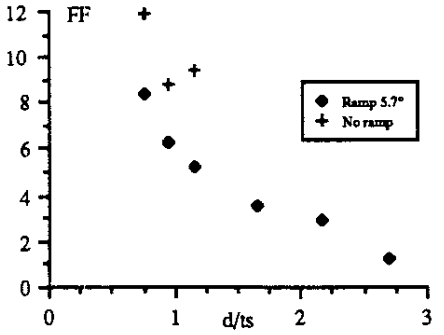

Fig. 17 FF versus the flow depth $\Delta(FF)/FF = \pm 10$ percent

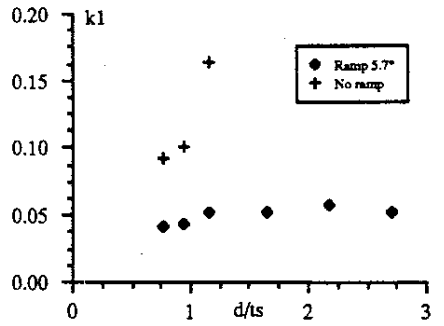

Fig. 18 k_1 versus the flow depth $\Delta(k_1)/k_1 = \pm 10$ percent

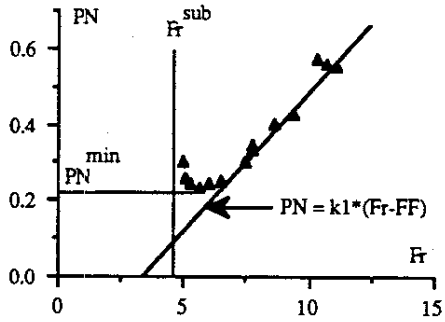

Fig. 19 Curve $P_N = f(Fr)$ for $Q_{air}^{inlet} = 0$—Ramp 5.7°—$d/t_s = 2.17$

Pa) the Fig. 14 indicates that, for a given pressure gradient and Froude number, the air discharge decreases when the ambient pressure above the jet P_o decreases. This suggests that the performances of aerator located at high altitude may be affected by the lower atmospheric pressure.

Laali (1980) then introduced artificial roughness (paper sand $k_s = 0.4$ mm) on the lower surface of the nozzle of the orifice in order to modify the free-surface irregularities of the jet and the experimental results are plotted in Fig. 15. The presence of roughness on the nozzle of the injector increases the thickness of the initial boundary layer and therefore reduces the height of the uniform turbulent flow. The results are then expected to be similar to the effects of a reduction of the jet thickness and this is observed on Fig. 15. Laali (1980) indicated that the effect of the roughness is less important for large Froude numbers as the boundary layer thickness is reduced as the Reynolds number increases.

Ervine and Falvey (1987) investigate the effect of turbulence on free jets discharging horizontally and suggest that some important processes in turbulent jets in the atmosphere are dependent on Weber and Reynolds numbers and the turbulence intensity Tu. Then great difficulties appear in modelling free jets and studies must be related to the equation (2).

4 Study of the Case $Q_{air} = 0$

4.1 Introduction. The flow above an aerator when $Q_{air}^{inlet} = 0$ is function of the spillway slope, the aerator geometry and the flow characteristics. At low Froude numbers or for low channel slopes the aerator is submerged when the air discharge is zero. For high channel slopes and high ramp slopes the cavity below the jet is not usually submerged when the air supply system is sealed. The transition between the two regimes corresponds to the conditions of submergence of the aerator. When the aerator is not submerged and for $Q_{air}^{inlet} = 0$, the cavity below the nappe is subject to air recirculation Chanson (1989).

4.2 Relationship $P_N = f(Fr)$. When the cavity is not submerged the cavity geometry (for $Q_{air}^{inlet} = 0$) is characterized by the nappe subpressure and the Froude number. Figure 16 present the author's data for various flow depths. The relationship $P_N = f(Fr)$ characterizes the behavior and the shape of the cavity when the air discharge supplied by the air inlets is zero.

The data show a good correlation. For high Froude numbers, the relationship $P_N = f(Fr)$ is almost linear and is estimated by:

$$P_N = k_1 * (Fr - FF) \tag{8}$$

The variations of the coefficients FF and k_1 are plotted on Figs. 17 and 18 versus the dimensionless depth of water for the Clyde dam spillway model.

4.3 Submergence of the Aerator. Under high subpressures the aerator becomes submerged and stops playing its protective role. For small Froude numbers and small air discharges an obstruction (partial or complete) of the air supply increases the pressure gradient above a limit and the aerator could be

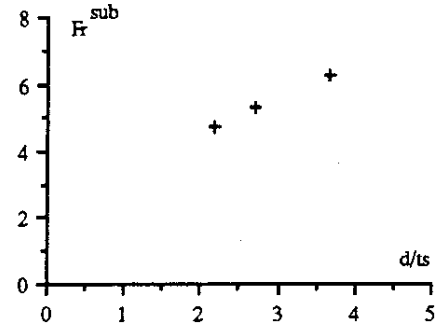

Fig. 20 Fr^{sub} as a function of the flow depth $\Delta(Fr^{sub})/Fr^{sub} = \pm 5$ percent

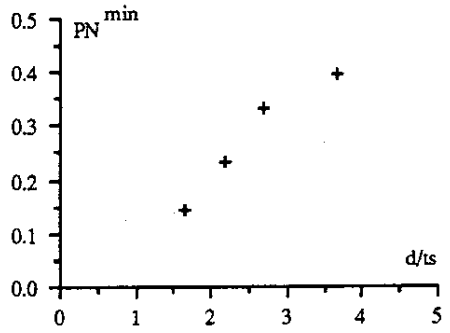

Fig. 21 P_N^{min} as a function of the flow depth $\Delta(P_N^{sub})/P_N^{sub} = \pm 2$ percent

submerged. When the cavity pressure drops the submergence is preceded by the appearance of a large amount of spray falling from the underside the nappe. The rear part of the jet is affected by rollers and the curvature of the jet is pronounced.

The study of the data $P_N = f(\mathrm{Fr})$ for $Q_{air}^{inlet} = 0$ highlights two characteristic parameters (Fig. 19): the submergence Froude number Fr^{sub} such that no submergence occurs for $Fr > Fr^{sub}$ and the minimum pressure gradient P_N^{min}. These parameters are function of the flow depth and the aerator geometry. For the aerator configuration with a 5.7° ramp the parameters Fr^{sub} and P_N^{min} are plotted in Figs. 20 and 21. For the aerator configuration without ramp the only information is: $Fr^{sub} > 15$ for $d/t_s = 1.65$ and $Fr^{sub} < 11$ for $d/t_s = 1.15$.

5 Conclusion

The study of the air demand is complex and the dimensional analysis shows that a similitude between model and prototype is almost impossible to respect. However the air demand provides a relationship between the air discharge, the subpressure and the flow characteristics, and for given flow conditions and aerator geometry the combination of the air demand characteristic curves and the pressure loss curve of the air supply system determinates the subpressure in the cavity beneath the jet and hence the jet trajectory. This enables the determination of the boundary conditions for a complete study of air entrainment above the aerator and the flow conditions downstream of the nappe. The air demand study provides additional informations. Indeed it highlights a characteristic Froude number above which nappe entrainment occurs. For smaller Froude numbers air entrainment occurs by plunging jet entrainment.

When the air inlets are sealed ($Q_{air}^{inlet} = 0$) the aerator is submerged for low Froude numbers. For high velocities the cavity beneath the nappe is clearly marked and the subpressure in the cavity and the cavity geometry is a function of the Froude number for given flow conditions and aerator geometry. The conditions for the disappearance of the cavity, called submergence, were obtained as a function of the initial flow depth for the aerator with ramp.

Acknowledgments

The author wishes to thank the Civil Engineering Department, University of Canterbury (New Zealand), the University Grant Committee (New Zealand) and the ministry of Works and Development (New Zealand) for their financial support. The author also thanks Professor I. R. Wood who supervised this project and Dr. J. M. Michel for his help.

References

Volkart, P., and Rutschmann, P., 1984, Air Entrainment Devices, Mitteilungen der Versuchsanstalt fur Wasserbau, Hydrologie und Glaziologie, No. 72, Zürich, Switzerland.

Peterka, A. J., 1953, "The Effect of Entrained Air on Cavitation Pitting," Joint Meeting Paper, IAHR/ASCE, Minneapolis, USA, Aug.

Russell, S. O., and Sheehan, G. J., 1974, "Effect of Entrained Air on Cavitation Damage," *Canadian Journal of Civil Engineering*, Vol. 1.

Vischer, D., Volkart, P., and Sigenthaler, A., 1987, "Hydraulic Modelling of Air Slots on Open Chute Spillways," Int. Conf. on Hyd. Modelling, BHRA Fluid Eng., Coventry, England, Sept.

Volkart, P., and Chervet, A., 1983, "Air Slots for Flow Aeration," Mitteilungen der Versuchsanstalt fur Wasserbau, Hydrologie und Glaziologie, No. 66, Zürich, Switzerland.

Chanson, H., 1989, "Study of Air Entrainment and Aeration Devices," *Jl. of Hyd. Res.*, Vol. 27, No. 3, pp. 301-319.

Low, H. S., 1986, "Model Studies of Clyde Dam Spillway Aerators," Master Report, Ref. 86-6, University of Canterbury, New Zealand.

Pinto, N. L. de S., Neidert, S. H., and Ota, J. J., 1982, "Aeration at High Velocity Flows," Water Power & Dam Construction, Feb.-Mar.

Tan, T. P., 1984, "Model Studies of Aerators on Spillway," Master Report, Ref. 84-6, University of Canterbury, New Zealand.

Chanson, H., 1988, "Study of Air Entrainment and Aeration Devices on Spillway Model," Research Report 8-88, University of Canterbury, New Zealand, Oct.

Laali, A. R., 1980, "Ecoulement Ventilés. Etude de l'entraînement d'air. Cas d'une cavité formée entre un jet plan et une paroi solide," Ph.D. thesis, University of Grenoble 1-INPG, France.

Ervine, D. A., and Falvey, H. T., 1987, "Behaviour of Turbulent Water Jets in the Atmosphere and in Plunge Pools," *Proc. Instn. Civ. Engrs.*, Part 2, 1984, 83, Mar., pp. 295-314.

Laali, A. R., and Michel, J. M., 1984, "Air Entrainment in Ventilated Cavities: Case of the Fully Developed Half-Cavity," ASME Journal of Fluids Engineering, Vol. 106, Sept. pp. 327-335.

Kobus, H., 1984, "Local Air Entrainment and Detrainment," *Symp. on Scale Effects in Modelling Hydraulic Structures*, IARH.

Michel, J. M., 1984, "Some Features on Water Flows with Ventilated Cavities," ASME Journal of Fluids Engineering, Vol. 106, Sept. pp. 319-326.

Pinto, N. L. de S., 1984, "Model Evaluation of Aerators in Shooting Flow," *Symp. on Scale Effects in Modelling Hydraulic Structures*, IARH.

Frizell, K. W., 1985, Glenn Canyon Dam Spillway Tests. Model-Prototype Comparison Hydraulics and Hydrology in the Small Computer Age, ASCE, New York.

Ervine, D. A., and Ahmed, A. A., 1982, "A Scaling Relatinship for a Two-Dimensional Dropshaft Hyd. Modelling of Civil Eng. Structures," BHRA Fluid Eng., Coventry, England.

Brauer, H., 1971, Grundlagen der Einphasenund Mehrphasenstromungen Verlag Sauerlander, Aarau and Frankfurt am Main.